Analyst

PAPER

View Article Online
View Journal | View Issue

Cite this: *Analyst*, 2014, **139**, 2193

An electrochemical sensing platform based on local repression of electrolyte diffusion for single-step, reagentless, sensitive detection of a sequence-specific DNA-binding protein†

Yun Zhang,* Fang Liu, Jinfang Nie,* Fuyang Jiang, Caibin Zhou, Jiani Yang, Jinlong Fan and Jianping Li

Received 14th January 2014
Accepted 13th February 2014

DOI: 10.1039/c4an00096j

www.rsc.org/analyst

In this paper, we report for the first time an electrochemical biosensor for single-step, reagentless, and picomolar detection of a sequence-specific DNA-binding protein using a double-stranded, electrode-bound DNA probe terminally modified with a redox active label close to the electrode surface. This new methodology is based upon local repression of electrolyte diffusion associated with protein–DNA binding that leads to reduction of the electrochemical response of the label. In the proof-of-concept study, the resulting electrochemical biosensor was quantitatively sensitive to the concentrations of the TATA binding protein (TBP, a model analyte) ranging from 40 pM to 25.4 nM with an estimated detection limit of ~10.6 pM (~80 to 400-fold improvement on the detection limit over previous electrochemical analytical systems).

Introduction

Sequence-specific DNA-binding proteins play an essential role in a variety of transcriptional regulatory networks including transcription, replication, recombination, and repair.[1,2] In particular, transcription factors, one of the largest classes of these proteins, are promising biomarkers in drug screening and new diagnostics of disease states,[3,4] since their signaling dysregulation is linked to many cancers, inflammation, autoimmunity, and developmental disorders.[5,6] The traditional toolbox for detection of DNA-binding proteins includes methods such as electrophoresis mobility shift,[7] DNA footprinting assay,[8] western blotting,[9] and enzyme-linked immunosorbent assay (ELISA).[10] Although successfully implemented in resource-rich settings, these methods are challenging for widespread use in common analytical laboratories, as they are cumbersome, time-consuming, or even radioactive.

In recent years, several alternative methods have been established, including the microarray chip,[11–13] electrochemical biosensor technique,[14–18] atomic force microscope imaging,[19] surface-enhanced resonance Raman scattering,[20] surface plasma resonance chip,[21] fluorescence resonance energy transferring measurement,[22] alternating laser excitation spectroscopy,[23] electrochemiluminescence sensor,[24] and colorimetric assay.[25] Each of these newer methods has its own advantages and disadvantages, but the electrochemical biosensor techniques that have evolved dramatically over the last decade benefit from many attractive features;[14–18,26–28] key among them are high detection sensitivity and specificity, simple instrumentation, and low endogenetic background. Such biosensors perform well in complex media such as cellular extracts,[14] blood serum,[29] and foodstuffs.[30] They are additionally easy to be miniaturized for the development of portable analytical devices to meet portability requirements of on-site screening or decentralized testing.[15,26,31]

Most electrochemical strategies of measuring the specific binding of the target protein to its DNA probe only incorporate the recognition event into the sensor design. For instance, the presence of the target protein is signaled through direct monitoring of electrochemical impedance.[14] Alternative designs exploit certain conformational changes of a DNA probe that modulates the distance of a redox active label (*e.g.*, methylene blue) modified at the middle or free terminal of the probe from the electrode and alters the redox current.[15,16] Another conceptually distinct mechanism is based on the electrochemistry of double-stranded DNA. The recognition affinity kinks the DNA duplex and perturbs the base pair stack, thus attenuating the DNA-mediated reduction of redox reporters such as Nile blue[17] and daunomycin[18] modified at the free terminal of the DNA away from the electrode surface. By using a double-stranded DNA probe terminally modified with a redox label close to the electrode surface, in this paper, we report the proof-of-principle of a novel electrochemical biosensor for sensitive detection of

College of Chemistry and Bioengineering, Guilin University of Technology, Guilin 541004, China. E-mail: zy_hnu@163.com; Niejinfang@glut.edu.cn; Fax: +86 773 5896839; Tel: +86 773 5896453

† Electronic supplementary information (ESI) available. See DOI: 10.1039/c4an00096j

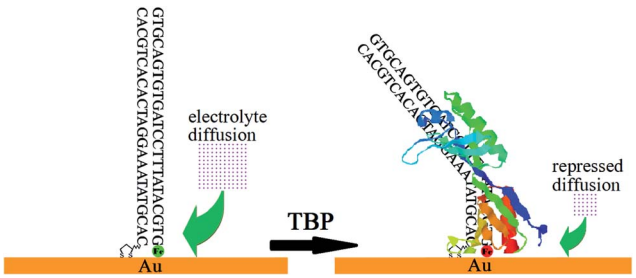

Fig. 1 Schematic illustration of the electrochemical TBP sensor that makes use of a double-stranded DNA probe terminally modified with a Fc redox label close to the gold electrode surface. Binding of the target TBP to its consensus sequence represses local diffusion of the electrolyte solution, followed by attenuation of the electrochemical response of Fc.

DNA binding proteins *via* local repression of electrolyte diffusion. This biosensor allows a single-step, reagentless, signal-off assay toward a model target, the TATA-binding protein (TBP) with high sensitivity and specificity. TBP is a key transcriptional factor involved in various important transcriptional regulatory networks that binds to a DNA sequence called the TATA box located in the core promoter regions of many genes.[32]

The new strategy proposed for TBP detection is schematically illustrated in Fig. 1. The recognition DNA probe used consists of two complementary strands incorporating the TBP binding site. The 5′ terminal of one strand was modified with thioctic acid and the 3′ terminal of the complementary strand was modified with ferrocene (Fc), a sort of redox active label that has been proved advantageous in developing excellent electrochemical detection systems.[33–35] The thiol- and Fc-modified strands were thermally annealed in equimolar amounts to form duplex DNA. A cleaned gold electrode was then immobilized with a stable self-assembled DNA monolayer *via* strong S–Au interactions. In the absence of the target protein, the Fc labels close to the electrode surface allow for production of a substantial redox current in 0.1 M $NaClO_4$. When TBP analytes bind to the specific sites in DNA probes, they not only kink the DNA duplex, but also repress local diffusion of the electrolyte from the bulk solution to the Fc label because of the steric bulk of the non-conductive target proteins, therefore lowering the electron transfer efficiency leading to reduced electrochemical response.

Experimental

Reagents

TATA binding protein (TBP) was obtained from Protein One Co., Ltd (Bethesda, Maryland, USA). Ferrocene (Fc) monocarboxylic acid, *N*-hydroxysulfosuccinimide (sulfo-NHS), 1-ethyl-3-(3-dimethylaminopropyl) carbodiimide hydrochloride (EDC), thioctic acid, mercaptohexanol (MCH), and full-length human p53 protein (P53) were from Sigma-Aldrich. Bovine serum albumin (BSA) and glucose oxidase (GOD) were provided by Dingguo Biotechnology Co., Ltd (Beijing, China). All other reagents of analytical grade were purchased from Sinopharm Chemical Reagent Co., Ltd (Shanghai, China) and used without further purification. All solutions were prepared with deionized water (with a specific resistivity >18.2 MΩ cm) from an ultrapure water system (UPS-II-20L) that was provided by Chengdu Yue Chun Technology Co., Ltd (Chengdu, China). The involved buffered solution was 10 mM phosphate-buffered saline (PBS, 10 mM phosphate buffer, 0.3 M NaCl, pH 7.4) solution.

The synthetic oligonucleotides used were ordered from Takara Biotechnology Co., Ltd (Dalian, China). The thermodynamic parameters of all oligonucleotides were calculated using bioinformatics software (http://mfold.rna.albany.edu/). The sequence of the sense strand 1 (S1) is 3′-CACG TCAC ACTA GG*AA ATAT* GCAC-5′-NH_2. The sequence of the complementary antisense strand 2 (S2) is 5′-GTGC AGTG TGAT CC*TT TATA* CGTG-3′-NH_2. The italic portions indicate the TATA protein-binding sites. Thioctic acid and Fc monocarboxylic acid are further covalently attached to the 5′ end of S1 and 3′ end of S2, respectively.

Apparatus and electrochemical measurements

Electrochemical experiments were carried out on a CHI 430B electrochemical workstation obtained from Shanghai Chenhua Instruments Inc. (Shanghai, China). A conventional three-electrode configuration was used, with a modified gold working electrode (2 mm in diameter), a platinum wire counter electrode, and a saturated calomel electrode (SCE) as the reference electrode. Cyclic voltammogram (CV) and differential pulse voltammogram (DPV) measurements were performed in 5 mL of 100 mM $NaClO_4$. DPV parameters were listed as follows: initial potential 600 mV, final potential 100 mV, increment potential 4 mV, pulse amplitude 50 mV, sample width 16.7 ms, pulse period 0.2 s, pulse width 0.05 s, quiet time 2 s, and sensitivity 10^{-7} A V^{-1}. CV scanning was carried out from −100 to 600 mV with a potential scanning rate of 100 mV s^{-1}. Moreover, electrochemical impedance spectroscopy (EIS) measurements were performed on an Autolab PGSTAT 128N electrochemical workstation. Impedance spectra were recorded over a voltage frequency range of 1 to 100 000 Hz at an initial potential of 240 mV with an alternating current potential amplitude of ±5 mV. The supporting electrolyte used for EIS was 10 mM PBS containing 100 mM KCl and a 5 mM $K_3[Fe(CN)_6]$ and $K_4[Fe(CN)_6]$ redox couple. All potentials were referred to SCE.

Fabrication of thiol- and fc-conjugated oligonucleotides

The conjugation of thioctic acid to S1 was carried out using the succinimide coupling (EDC-NHS) method.[33,34] Briefly, 100 μL of 10 μM S1 solution was mixed with 1 mL of 10 mM PBS (pH 7.4) containing 10 mM thioctic acid, 1 mM EDC, and 5 mM sulfo-NHS and incubated at 37 °C for ~2 h. The conjugate was dialyzed against 10 mM PBS (500 mL) for ~3 days in the dark to remove excessive thioctic acid. Moreover, the conjugation of Fc monocarboxylic acid to S2 was conducted according to a literature method with a minor modification.[35] Briefly, 1 mg of Fc monocarboxylic acid was added to 1 mL of 10 mM PBS (pH 7.4) containing EDC/NHS (0.1 M each) solution and immediately mixed. After 100 μL of 10 μM S2 solution was injected, the resulting solution was stirred at room temperature for ~2 h, and subsequently stored at 4 °C for further use.

Pretreatment of the gold electrode

First of all, gold electrodes were polished with 0.3 and 0.05 μm aluminum slurry and sonicated sequentially in distilled water, ethanol and distilled water for ~5 min each. The polished electrodes were then immersed in a fresh warm piranha solution (volume (concentrated sulfuric acid)/volume (30% peroxide solution) = 3 : 1) for ~15 min. After they were rinsed thoroughly with deionized water, these gold electrodes were further electrochemically cleaned in 0.1 M H_2SO_4 with potential scanning from 200 to 1600 mV until a remarkable voltammetric peak was obtained, followed by another sonication treatment and drying with nitrogen.

Biosensor fabrication and sample assay

Prior to biosensor fabrication, the thiol- and Fc-modified oligonucleotides were mixed in equimolar amounts. The mixture was heated to 70 °C and incubated for ~10 min, followed by cooling to room temperature (over 2 h). Such treatment resulted in the formation of duplex DNA probes *via* the hybridization of the two sorts of labeled oligonucleotides. The fabrication of the electronic sensing interface was accomplished by the S–Au self-assembly. Briefly, a droplet of 20 μL duplex DNA probe (1.6 μM) was cast onto the pretreated electrode and incubated at room temperature for ~2 h in humidity. Then, the electrode surface was rinsed with deionized water and blocked with 1 mM MCH for ~10 min. After washing with PBS to remove the physically adsorbed molecules, the modified electrode was ready for TBP detection. The DNA-modified gold electrode was soaked in 10 μL TBP sample solution at various concentrations at 37 °C for ~1 h, followed by another washing treatment for subsequent electrochemical measurements. The current change was defined as $(I_s - I_c)$, where I_s and I_c were the DPV peak currents after soaking the DNA modified electrode in PBS containing the TBP analyte and in PBS in the absence of TBP, respectively, and used to estimate the amount of TBP in the sample. Selectivity experiments were also performed in the same fashion but using P53, BSA, and GOD instead of TBP.

Results and discussion

CV and DPV characterization of the TBP biosensor

The electrode modified with a self-assembled DNA monolayer (~1.14×10^{13} molecules per cm^2, see detailed calculation in the ESI†)[17,34] demonstrated a signal-off architecture in response to the target. In the absence of TBP, CV showed a pair of well-defined current peaks at 195 and 298 mV (Fig. 2A, curve a), a typical redox peak range of the Fc label.[33] This suggests successful immobilization of Fc-tagged DNA probes on the gold surface. After reaction with 25.4 nM TBP, as expected, significant reduction of the signal was observed in the CV (Fig. 2A, curve b), evidencing the feasibility of the electrical assay system for TBP screening *via* the strategy of analyte-repressed local electrolyte diffusion. DPVs provided quite nice resolution of the binding response (Fig. 2B). One observed a large DPV peak around 293 mV in the absence of the target protein, which was due to the high electron transfer efficiency of the redox reporter placed close to the electrode surface. The reaction with 25.4 nM TBP

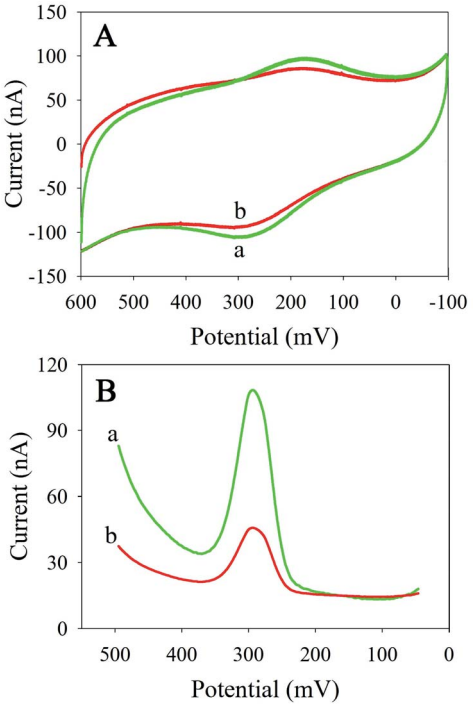

Fig. 2 (A) CVs of the developed biosensor after reactions with (a) blank PBS sample and (b) 25.4 nM TBP. (B) Corresponding DPVs.

resulted in a significant change of the DPV peak current with a signal reduction of ~68.2% with reference to that for the blank (Fig. 2B). In contrast, other proteins (1 μM), namely P53, BSA, and GOD did not produce significant alterations of DPV signals (Fig. 3), indicating that the as-fabricated biosensor was not responsive to non-specific interactions between these proteins and the modified DNA probes. Moreover, it should be pointed out that the TATA box in the DNA probe should be as close as possible to the electrode for facilitating the TBP-repressed local electrolyte diffusion from the bulk solution to the Fc redox label. The DNA probe that contains four pairs of non-specific bases between the 5′ end of the thiol-modified strand and the TATA box was optimized for use in the current work for specific recognition of the target protein (Fig. S1 in the ESI†).

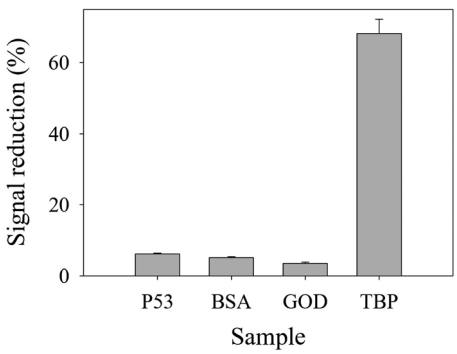

Fig. 3 DPV peak current changes for different proteins (TBP, 25.4 nM; other proteins, 1 μM) with reference to the blank. Each error bar represents a standard deviation across five repetitive experiments.

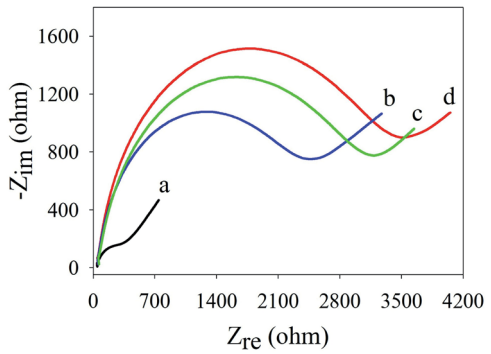

Fig. 4 Nyquist plots ($-Z_{im}$ *vs.* Z_{re}) for Faradaic impedance spectra obtained at different electrodes: (a) bare gold electrode, (b) DNA-immobilized electrode, (c) MCH-blocked electrode, and (d) TBP-bound electrode.

Impedance characterization of the biosensor fabrication

In order to characterize the fabrication process of the TBP sensor, electrochemical impedance spectroscopy measurement was carried out.[14] The resultant Faradaic impedance spectra (presented as Nyquist plots) are displayed in Fig. 4. As the redox couple of $[Fe(CN)_6]^{3-/4-}$ is sensitive to surface chemistry,[36] it was engaged to indicate the electrochemical behaviors of the sensor at different fabrication stages. Very small impedance is observed on the bare gold electrode (curve a). After the immobilization of thiolated DNA probes and surface blocking with MCH, the impedances (curves b and c) on the electrode increase remarkably, suggesting the successful formation of self-assembled layers on the gold surface. The lower electron transfer efficiency may be mainly attributed to the fact that the negative charges on the DNA backbone and MCH repel $[Fe(CN)_6]^{3-/4-}$ from the modified electrode. Moreover, the impedance response increases further after the binding of TBP to DNA (curve d), due to the introduction of the non-conductive target proteins with steric bulk serving as more electron transfer barriers.

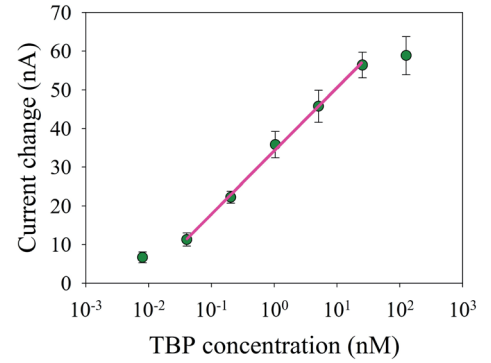

Fig. 5 Peak current changes in DPVs for the sensing interfaces upon the addition of TBP at different concentrations ranging from 8 pM to 126 nM with reference to the blank. The colour calibration curve corresponding to the electrochemical detection of various TBP concentrations. The current change value is linearly related to the target protein concentration in the range of 40 pM–25.4 nM. Each data point represents the average value of five repetitive experiments. Error bars reflect the standard deviations from the average values.

Analytical performance

The main experimental factors for the proposed biosensor have been studied in detail, including the concentration and incubation time for DNA immobilization and the reaction temperature and time for the DNA–protein binding (Fig. S2–S5 in the ESI†). To study its quantitative analytical capability, a series of TBP samples with varying analyte concentrations in the range of 8 pM–126 nM were assayed under optimized conditions. It is clearly observed from Fig. 5 that as the TBP concentration increases, the DPV peak current change increases, indicating the analyte-controlled electrochemical response of the Fc label. As shown in Fig. 5 that further displays a calibration curve describing the relationship between the current changes and the TBP concentrations, the linear detection range was found to be 40 pM–25.4 nM (R^2 = 0.9980), with an estimated detection limit of ~10.6 pM (3σ).

This new biosensor technique achieves comparable or even better sensitivity against some previously reported TBP detection schemes listed in Table 1. From this table, one can see that the present work on TBP assay using electrodes immobilized with DNA containing a redox label close to the electrode surfaces shows ~80 to 400-fold improvement on the limit of detection over other previous electrochemical detection systems coupled with DNA probes tagged with redox active reporters away from the electrode surfaces.[14–17] Our method, which is free of any amplification process, also exhibits ~2 to 1000-fold improvement on the detection limit against other TBP assay schemes that utilized DNA-conjugated gold nanoparticles[20,25] or potassium-doped graphene and SiO_2@CdS nanocomposites[24] for signal amplification.

Measurement reproducibility

The measurement reproducibility was also studied by evaluating the intra- and inter-assay precision of the peak current recorded in DPV. Three TBP samples of various concentrations (*i.e.*, 0.202, 5.04, and 25.4 nM) within the dynamic range were analyzed. The intra-assay precision was estimated from five repetitive assays of one sample using the same gold electrode, while the inter-assay precision was assessed *via* the analysis of the same sample with four different electrodes. The maximum relative standard deviation was ~9.62% and ~10.8% for the intra- and inter-assay, respectively, demonstrating acceptable measurement reproducibility of this propped detection system. It seems that the major sources of these signal variations are hands-on operations in the sensor fabrication and testing protocol, and/or the difference of the surface areas from electrode to electrode.

Recovery experiment

To further assess the applicability and reliability of the biosensor, the recovery experiments of several TBP samples at set concentrations within the linear range were conducted. A certain

Table 1 Comparison of the proposed TBP biosensor with some reported detection techniques

Detection technique	Limit of detection (nM)	Linear range (nM)	Ref.
Electrochemical impedance spectroscopy technique using an electrode-bound DNA probe without a redox label	0.8	0.8–68.8	14
SWV method with an electrode-bound DNA probe modified with a redox tag at its middle[a]	3	~30 to 1000	15
SWV assay with an electrode-bound DNA probe modified with a redox label at its middle or free terminal away from the electrode	2	~2 to 12	16
SWV technique with an electrode-bound DNA probe modified with a redox tag at its free terminal away from the electrode	4	NA[b]	17
DPV biosensor with an electrode-bound DNA probe modified with a redox label at its terminal close to the electrode	0.0106	0.04–25.4	This work
Surface enhanced resonance Raman scattering technique with DNA-modified gold nanoparticles	1	1–80	20
Electrochemiluminescence biosensor with DNA-modified potassium-doped graphene and SiO_2@CdS nanocomposites	0.02	0.2–100	24
Colorimetric assay with DNA-modified gold nanoparticles	10	10–120	25

[a] SWV, square wave voltammetry. [b] NA, not available.

amount of sample with a given analyte concentration was added into a blank sample resulting in the final TBP concentration of 0.202, 5.04, or 25.4 nM. The DPV measurements were performed according to the general procedures, and the "Found" concentrations were estimated from the corresponding current changes using the regression equation. All the measurements were carried out three times. As shown in Table S1 in the ESI,† the obtained recovery results are in the range of ~94.5 to 106%, and the average relative standard deviation is ~8.31%.

Conclusions

We have demonstrated the construction of a highly sensitive electrochemical biosensor for detecting a TBP model analyte at a picomolar level, using a double-stranded, electrode-bound DNA probe terminally modified with a redox label close to the electrode surface. This methodology relies on the locally repressed electrolyte diffusion associated with the protein–DNA binding that leads to reduction in the electrochemical response of the redox label. This new electrochemical assay approach may provide a convenient platform for developing biosensors with high performance in sensitive and selective detection of proteins that are able to bind double-stranded DNA. With different redox-tagged DNA probes, each specifically designed for individual proteins, it is possible to extend this strategy to multiplex detection of multiple proteins in a densely packed sensing array format, on which some studies are now underway in our group.

Acknowledgements

The authors gratefully acknowledge the financial support from the National Natural Science Foundation of China (Grant nos 21105017, 21205021, and 21365009) and the Guangxi Natural Science Foundation (Grant nos 2012GXNSFBA053030 and 2012GXNSFBA053029).

Notes and references

1 B. Ren, F. Robert, J. J. Wyrick, O. Aparicio, E. G. Jennings, I. J. Zeitlinger, J. Schreiber, N. Hannett, E. Kanin, T. L. Volkert, C. J. Wilson and S. P. Bell, *Science*, 2000, **290**, 2306–2309.
2 K. Helin, *Curr. Opin. Genet. Dev.*, 1998, **8**, 28–35.
3 P. P. Pandolfi, *Oncogene*, 2001, **20**, 3116–3127.
4 D. Sikder and T. Kodadek, *Curr. Opin. Chem. Biol.*, 2005, **9**, 38–45.
5 J. E. Darnell Jr, *Nat. Rev. Cancer*, 2002, **2**, 740–749.
6 T. A. Libermann and L. F. Zerbini, *Curr. Gene Ther.*, 2006, **6**, 17–33.
7 M. M. Garner and A. Revzin, *Nucleic Acids Res.*, 1981, **9**, 3047–3060.
8 D. J. Galas and A. Schmitz, *Nucleic Acids Res.*, 1978, **5**, 3157–3170.
9 B. Bowen, J. Steinberg, U. K. Laemmli and H. Weintraub, *Nucleic Acids Res.*, 1980, **8**, 1–20.
10 P. Renard, I. Ernest, A. Houbion, M. Art, H. Le Calvez, M. Raes and J. Remacle, *Nucleic Acids Res.*, 2001, **29**, e21.
11 M. L. Bulyk, *Curr. Opin. Biotechnol.*, 2006, **17**, 422–430.
12 M. L. Bulyk, M. F. Berger, A. A. Philippakis, A. M. Qureshi, F. S. He and P. W. Estep, *Nat. Biotechnol.*, 2006, **24**, 1429–1435.
13 J. Wang, D. Onoshima, M. Aki, Y. Okamoto, N. Kaji, M. Tokeshi and Y. Baba, *Anal. Chem.*, 2011, **83**, 3528–3532.
14 H. Chang and J. Li, *Electrochem. Commun.*, 2009, **11**, 2101–2104.
15 A. J. Bonham, K. Hsieh, B. S. Ferguson, A. Vallée-Bélisle, F. Ricci, H. T. Soh and K. W. Plaxco, *J. Am. Chem. Soc.*, 2012, **134**, 3346–3348.
16 F. Ricci, A. J. Bonham, A. C. Mason, N. O. Reich and K. W. Plaxco, *Anal. Chem.*, 2009, **81**, 1608–1614.
17 A. Gorodetsky, A. Ebrahim and J. K. Barton, *J. Am. Chem. Soc.*, 2008, **130**, 2924–2925.

18 E. M. Boon, J. E. Salas and J. K. Barton, *Nat. Biotechnol.*, 2002, **20**, 282–286.
19 M. Menotta, R. Crinelli, E. Carloni, M. Bianchi, E. Giacomini, U. Valbusa and M. Magnani, *Biosens. Bioelectron.*, 2010, **25**, 2490–2496.
20 N. O. Reich, A. J. Bonham, G. Braun, I. Pavel and M. Moskovits, *J. Am. Chem. Soc.*, 2007, **129**, 14572–14573.
21 Y. C. Wang, X. Zhu, M. H. Wu, N. Xia, J. X. Wang and F. M. Zhou, *Anal. Chem.*, 2009, **81**, 8441–8446.
22 X. F. Liu, L. Ouyang, X. H. Cai, Y. Q. Huang, X. M. Feng, Q. L. Fan and W. Huang, *Biosens. Bioelectron.*, 2013, **41**, 218–224.
23 K. Lymperopoulos, R. Crawford, J. P. Torella, M. Heilemann, L. C. Hwang, S. J. Holden and A. N. Kapanidis, *Angew. Chem., Int. Ed.*, 2010, **49**, 1316–1320.
24 J. Wang, W. W. Zhao, X. R. Li, J. J. Xu and H. Y. Chen, *Chem. Commun.*, 2012, **48**, 6429–6431.
25 L. J. Ou, P. Y. Jin, X. Chu, J. H. Jiang and R. Q. Yu, *Anal. Chem.*, 2010, **82**, 6015–6024.
26 A. L. Liu, K. Wang, S. H. Weng, Y. Lei, L. Q. Lin, W. Chen, X. H. Lin and Y. Z. Chen, *Trends Anal. Chem.*, 2012, **37**, 101–111.
27 J. C. Vidal, L. Bonel, A. Ezquerra, S. Hernández, J. R. Bertolín, C. Cubel and J. R. Castillo, *Biosens. Bioelectron.*, 2013, **49**, 146–158.
28 E. Hamidi-Asl, I. Palchetti, E. Hasheminejad and M. Mascini, *Talanta*, 2013, **115**, 74–83.
29 B. R. Baker, R. Y. Lai, M. S. Wood, E. H. Doctor, A. J. Heeger and K. W. Plaxco, *J. Am. Chem. Soc.*, 2006, **128**, 3138–3139.
30 K. J. Cash, F. Ricci and K. W. Plaxco, *J. Am. Chem. Soc.*, 2009, **131**, 6955–6957.
31 Y. Wan, Y. Su, X. H. Zhu, G. Liu and C. H. Fan, *Biosens. Bioelectron.*, 2013, **47**, 1–11.
32 R. H. Blair, J. A. Goodrich and J. F. Kugel, *Biochemistry*, 2012, **51**, 7444–7455.
33 Y. Huang, Y. L. Zhang, X. Xu, J. H. Jiang, G. L. Shen and R. Q. Yu, *J. Am. Chem. Soc.*, 2009, **131**, 2478–2480.
34 Y. L. Zhang, Y. Huang, J. H Jiang, G. L. Shen and R. Q. Yu, *J. Am. Chem. Soc.*, 2007, **129**, 15448–15449.
35 S. B. Zhang, R. Hu, P. Hu, Z. S. Wu, G. L. Shen and R. Q. Yu, *Nucleic Acids Res.*, 2010, **38**, e185.
36 Y. Zhang, H. Wang, J. F. Nie, Y. W. Zhang, G. L. Shen and R. Q. Yu, *Biosens. Bioelectron.*, 2009, **25**, 34–40.